

APPLIED BEHAVIOR ANALYSIS OF NORTON AND THEVENIN CIRCUITS

Dumitru CIOFLICA, Adrian TULBURE and Calin PETRASCU
Department of Science and Engineering, "1 Decembrie 1918" University of Alba Iulia
N. Iorga No.11-13, 510009 Alba Iulia,
aditulbure@uab.ro

Abstract: The electromagnetic field theory uses the term „state” of the field, while the electronics circuits theory operates with the term „operation mode/regime” of the circuit. In the proposed paper the authors analyze two transient regimes, that take place in the current operation of the power grids: a) reducing the magnetic field of excitation circuit at the synchronous machine, assimilated to the coil discharging on a no-load grid and b) current supplying on an electric line with load, assimilated to the capacitor discharging on the connected consumers.

Starting from the standard basic models, the mentioned systems are mathematically modeled and simulated in MATLAB and LTSpice in three variants: aperiodical, periodical and critical mode. At the end of the paper a comparative evolution of the state variables $u(t)$, $i(t)$ at the dipoles terminals in different transient regimes is presented. The waveforms were experimentally validated by measurements on the test bench.

Keywords: power supply system, modeling-simulation, transient regime, Norton and Thevenin schemes, practical validation

I. PROBLEM DESIGN

The *operation mode* and *operation state* are two frequently used technical terms. The usual electric circuits can operate in 2 states, stationary or transition regimes. The state of the vacuum field can be: static (electrical), stationary (magnetical) and non-stationary (electro-magnetical radiation). The electromagnetic radiation generation in transition mode is theoretically possible, but is practically unlikely due to the real electric parameters.

This contribution aims to clarify two possible practical situations: dimming the excitation field on the synchronous machine and voltage application on the power line with load. The concrete situations are described below.

The basic mode of operation of the synchronous machine is the generator regime. This variant is the economic basis of electricity generation in all modern power plants. The rotor generates a constant magnetic field with the help of the permanent magnets or of the dc-current which is fed symmetric coils [1].

The self-resonance phenomenon of the SM occurs when, the under-excited synchronous machine in the generator mode is connected to the capacitive load (no load electric line, fig.1).

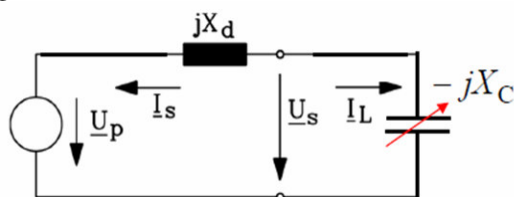


Figure 1. Synchronous machine on capacitive load [1]

The hysteresis in the magnets induces a low pole voltage ($U_p \sim 0$). This pole voltage can increase by the input of inductive current I_s , - generating a Ferranti effect in this way.

The operation is characterized by the following absolute and relative parameters:

$$\frac{U_s}{U_p} = 1 + \frac{I_s}{X_d} \quad (1) \quad u = 1 + i \quad (2)$$

Practically the no-load operation occurs if at one end of the line the voltage has a nominal value, while on the other no load is connected– e.g. due to the fault situation in the connected consumer or when a low load is powered (e.g. night charging).

In the second case, because of the power lines it is desirable to operate symmetrically (uniformly distributed load) and it is sufficient to determine the state parameters of a single phase [2].

For the analyzed system (power transmission line) a one phase representation is sufficient, as in the figure below.

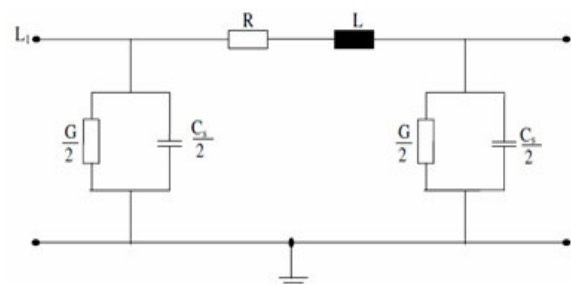


Figure 2. Symmetrically power line diagram [3]

II. THE BASIC MODELS

In order to build a mathematical model, an electric coil can be assimilated like a voltage source in series with an L, r group, as in fig.3.

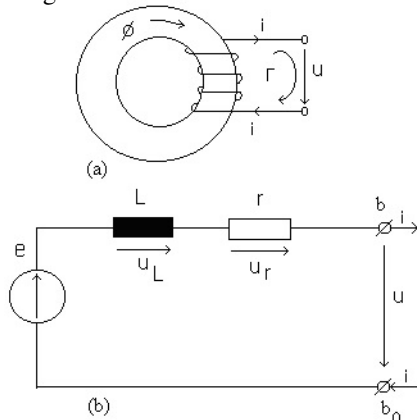


Figure 3. Electrical Coil –Model 1 (a) and Thevenin equivalent diagram (b)

Similarly, an electric capacitor can be replaced with a current source in parallel with a C, G group as in fig.4.

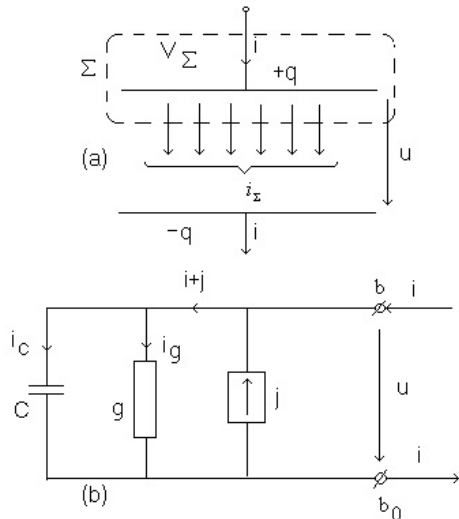


Figure 4. Electrical Capacitor –model 2 (a) and Norton equivalent diagram (b)

In both cases the real network is replaced with the simplified equivalent one. [4]. Finally, a circuit consisting of elementary electrical dipoles with sources, resistors, coils and capacitors like in fig.5 and 6 is obtained.

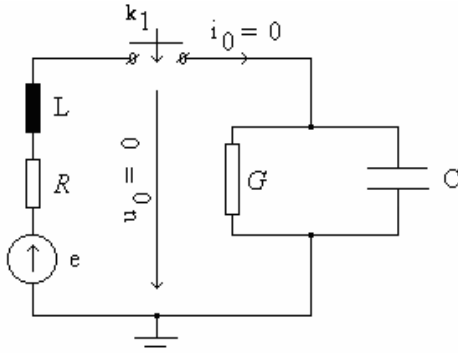


Figure 5. Equivalent diagram for model 1. [k1 - open].

In most cases, the variation of the state variables $u(t)$ and $i(t)$ should be known even from the design task.

For a unitary analysis, the following procedure can be adopted: generator convention for coil and receiver convention for the capacitor/consumer (model 1 / fig.5), respectively, the generator convention for capacitor and the receiver convention for coil/consumer (model 2 / fig.6).

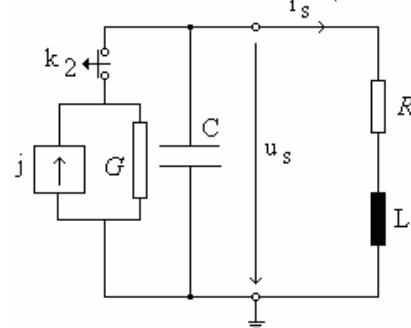


Figure 6. Equivalent diagram for model 2. [k2 - closed].

For the first topology we consider $j = 0$ and the initial conditions $u(0) = 0, i(0) = 0$.

Both equations (3) describe the behavior of model 1:

$$\begin{cases} (sC + G)U - I = 0 \\ U + (sL + R)I = E \end{cases} \quad (3)$$

The second topology is described by the equations (4) under non zero initial conditions $u(0) = u_s, i(0) = i_s$ and $e = 0$:

$$\begin{cases} (sC + G)U + I = sCu_s \\ -U + (sL + R)I = sLi_s \end{cases} \quad (4)$$

Using these mathematical models two transient regimes related to the power grid operations are analyzed: 1) coil discharging or excitation field reduction by the synchronous machine and voltage application to a no load power line and 2) capacitor discharging and voltage application to a power line with connected consumers.

III. THE SIMULATION RESULTS

For mathematical modeling, the Carson-transform, which has some advantages over Laplace-transform, is used. (The difference is the presence of the s operator [5]). The variable functions $\varphi(t), y(t), z(t)$ are expressed using the development theorem. For each case, the variation of time variant values at the terminals is computed using the following relations (i.e. $u(t)$ and $i(t)$ for model 1, fig.5):

$$u(t) = \varphi(t) \cdot e_0 \quad (5) \quad i(t) = y(t) \cdot e_0 \quad (6)$$

where:

$$\varphi(t) = \frac{1}{1 + RG} + \frac{1}{2LC} \left[\frac{e^{s_1 t}}{s_1(s_1 + \alpha)} + \frac{e^{s_2 t}}{s_2(s_2 + \alpha)} \right] \quad (7)$$

and

$$y(t) = G \cdot \varphi(t) + \frac{1}{L} \cdot \frac{e^{s_1 t} - e^{s_2 t}}{s_1 - s_2} \quad (8)$$

Similarly, the values $u(t)$ and $i(t)$ for model 2, (fig.6), are calculated by the following relations:

$$u(t) = -z(t) \cdot i_s \quad (9) \quad i(t) = \varphi(t) \cdot i_s \quad (10)$$

where:

$$z(t) = \frac{1}{C} \cdot \frac{e^{s_1 t} - e^{s_2 t}}{s_1 - s_2} \quad (11)$$

$$\varphi(t) = G \cdot z(t) + \frac{s_1 \cdot e^{s_1 t} - s_2 \cdot e^{s_2 t}}{s_1 - s_2} \quad (12)$$

These relationships are customized for following models:

- aperiodical: $\alpha > \beta$ and $s_{1,2} = -\alpha \pm \sqrt{\alpha^2 - \beta^2}$ (13)

- periodical: $\alpha = \beta$ and $(s_1 = s_2 = s_{cr} = -\alpha)$; $\alpha = \beta$ (14)

and the critical one ($\alpha < \beta$ $s_{1,2} = -\alpha \pm j\sqrt{\beta^2 - \alpha^2}$) (15)

By implementing the above relationships in the MATLAB simulation environment [6], the following diagrams: for capacitor charging - model 1 (fig.7) and for capacitor-discharging – model 2 (fig.8) are obtained.

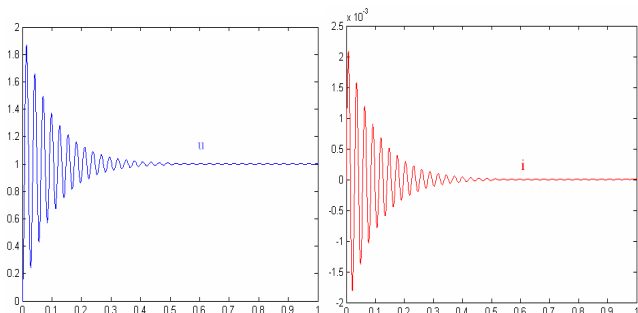


Figure 7. Voltage and current waveforms at C charging (Matlab periodical model $\alpha=10s^{-1}$ and $\beta=224s^{-1}$)

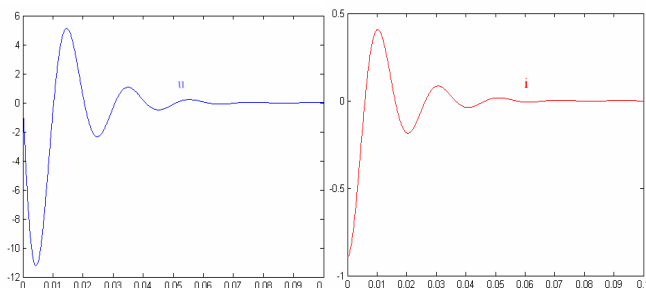


Figure 8. Voltage and current waveforms at C discharging (Matlab periodical model $\alpha=77s^{-1}$ and $\beta=317s^{-1}$)

After customizing these formulas we obtain the waveforms, valid for:

a) capacitor charging (fig.7)

- prescribed values: $e_0 = 1V, j = 0A$,
- initial values at $t = 0$: $i_0=0, u_0 = 0$,

- and final values: $u_{\infty} = \frac{e_0}{1 + RG}$; $i_{\infty} = \frac{G \cdot e_0}{1 + RG}$ (16)

b) capacitor discharging (fig.8)

- prescribed values: $i_s = 1A, e = 0V$,

- initial values at $t = 0$: $u_s = \frac{R \cdot j_s}{1 + RG}$ $i_s = \frac{j_s}{1 + RG}$ (17)

- and final values: $i_{\infty}=0, u_{\infty} = 0$

Similarly, one can proceed to obtain the other $u(t)$ and $i(t)$ values, for some α, β or R, L, C, G parameters [7].

IV. PRACTICAL VALIDATION

In order to confirm the analyzed phenomena, the structure

from figure 9 was used. An intermediate step consists of running the program in the LT-Spice environment [8]. The value for C_1 and L_1 is standard for an electric cable line of few km. The value for G is approximately for a tangent of the loss angle $tg\delta \approx 0.0025$ to 50 Hz.

Table 1. Parameters set in experiments

	C_1 [nF]	L_1 [mH]	G [nS]	R [Ω]
periodical	416	0,938	326	15
critical	416	0,938	326	95
aperiodical	416	0,938	326	215

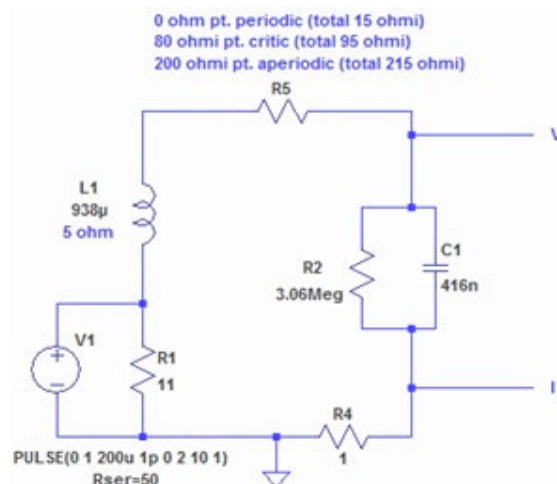


Figure 9. Equivalent diagram of the test circuit

The simulation results validate the correspondence between the electrical networks theory and the energy transfer and aspects of electromagnetic environment pollution. The graphs in the figures below were obtained by adjusting the component values according to the table 1.

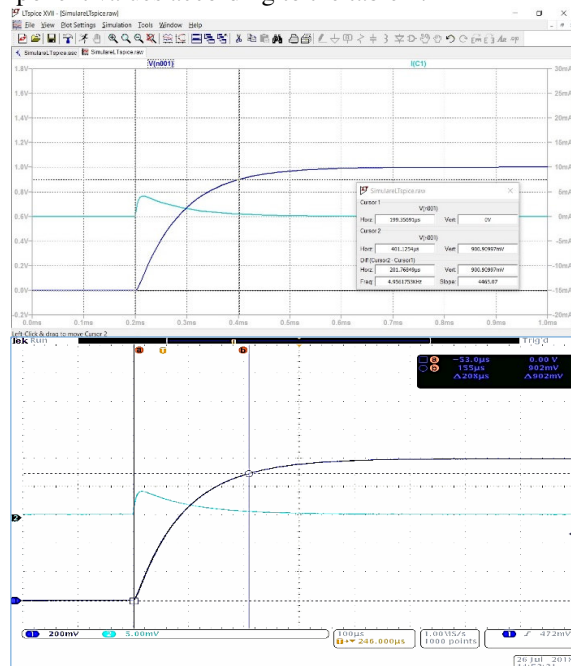


Figure 10. Voltage and current waveforms during C-charging for aperiodical model (top- LTSpice simulation with dynamic models and bottom-measurement)

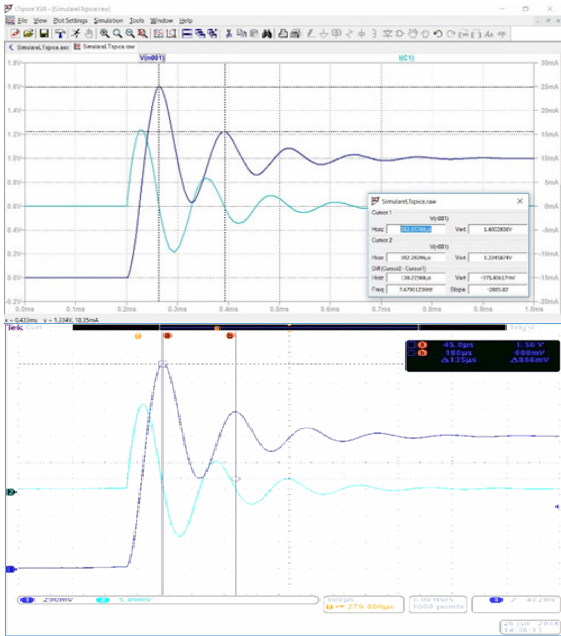


Figure 11. Voltage and current waveforms by C-charging for periodical model (top-digital LTSpice simulation with dynamic models and bottom-measurement)

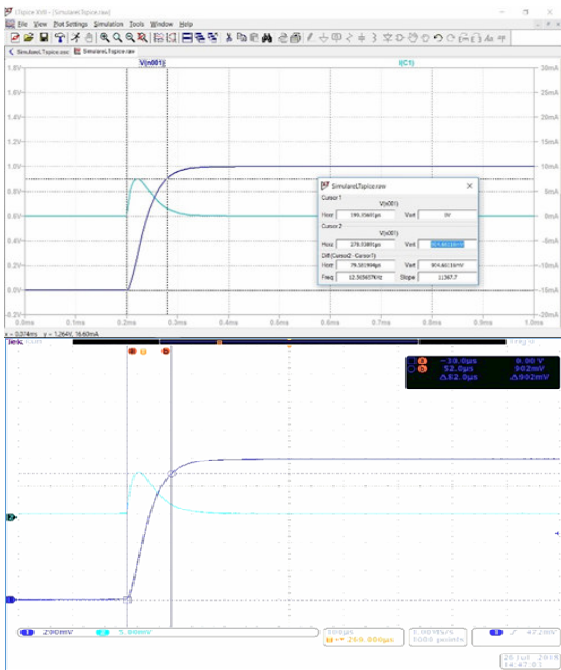


Figure 12. Voltage and current waveforms by C-charging for critical model (top-digital LTSpice simulation with dynamic models and bottom-measurement)

The transversal active power losses (represented by the parallel conductivity G) are estimated through the loss angle tangent (involving the capacitive reactance X_C at 50 Hz). They are mainly due to ionization around the cables and the dielectric hysteresis phenomena.

In order to validate the proposed theory, the test bench from figure 13 consisting of memory oscilloscope, signal generator, digital multimeter, DUT, shunts and measuring probes was built and used in laboratory.

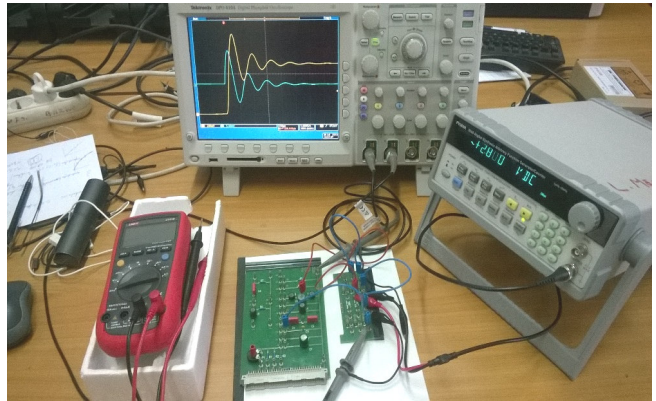


Figure 13. Measurement set-up

V. CONCLUSIONS

In the case of the analyzed transient phenomena (with a much lower voltage variation velocity between two conductors, than the one in the 50 Hz sinusoidal operation), the transversal conductivity may have different values than those considered in the calculations. However, they have low influence on the transient regime, so they can be neglected.

Given by the different time constants occurring at the starting time in the transient regime ($f_{grid}=50\text{Hz}$, $f_{trans}=6\text{kHz}$, fig.10-12), the model 1 can be assimilated to the synchronous generator linked to the no-load network. (night load, stand-by load).

Similarly, the second model can be assimilated in the practice to the situation when disconnecting the supply of a power line while keeping the ohmic-inductive consumers.

REFERENCES

- [1] A. Binder, „Elektrische Maschinen und Antriebe“. *Vorlesung am Institut für Elektrische Energieumwandlung* der TU Darmstadt. Darmstadt 2010.
- [2] M.F. Schönitzer, “Physikalische Grundlagen der Energieübertragung mit Gleich- und Wechselstrom hoher Spannung“ https://upload.wikimedia.org/wikipedia/commons/3/34/Physikalische_Grundlagen_der_Energie%C3%BCbertragung.pdf -2012
- [3] D. Rusinaru – “Scheme echivalente si parametrii liniilor electrice”. Curs Univ. Craiova 2010.
- [4] E.Potolea, D.Cioflica, M.Sănduleac, M. Trușia, ”Bazele fizice ale energiei”, Editura POLITEHNICA PRES, București, 2014.
- [5] Stover, Christopher. "Laplace-Carson Transform." *From MathWorld-A Wolfram Web Resource*, created by Eric W. Weisstein. <http://mathworld.wolfram.com/Laplace-Carson Transform.html>
- [6] William J. Palm. “Introduction to MATLAB for Engineers” McGraw-Hill Education 2010.
- [7] Fărcaș C., Petreuş D., Ciocan I., Palaghiță N., Modeling and Simulation of Supercapacitors, 15th International Symposium for Design and Technology of Electronics Packages – SIITME 2009, Gyula, Hungary, 2009, pp. 195 – 200, ISBN 978-1-4244-5132-6.
- [8] Gilles Brocard “The LTSpice IV Simulator: Manual, Methods and Applications” ISBN 978-3899292. Würth Elektronik 2013.